

Altered recognition of antigen is a mechanism of CD8⁺ T cell tolerance in cancer

Srinivas Nagaraj¹, Kapil Gupta², Vladimir Pisarev³, Leo Kinarsky³, Simon Sherman³, Loveleen Kang¹, Donna L Herber¹, Jonathan Schneck² & Dmitry I Gabrilovich¹

Antigen-specific CD8⁺ T-cell tolerance, induced by myeloid-derived suppressor cells (MDSCs), is one of the main mechanisms of tumor escape. Using *in vivo* models, we show here that MDSCs directly disrupt the binding of specific peptide–major histocompatibility complex (pMHC) dimers to CD8-expressing T cells through nitration of tyrosines in a T-cell receptor (TCR)–CD8 complex. This process makes CD8-expressing T cells unable to bind pMHC and to respond to the specific peptide, although they retain their ability to respond to nonspecific stimulation. Nitration of TCR–CD8 is induced by MDSCs through hyperproduction of reactive oxygen species and peroxynitrite during direct cell–cell contact. Molecular modeling suggests specific sites of nitration that might affect the conformational flexibility of TCR–CD8 and its interaction with pMHC. These data identify a previously unknown mechanism of T-cell tolerance in cancer that is also pertinent to many pathological conditions associated with accumulation of MDSCs.

T-cell tolerance plays an important part in tumor escape¹ and is one of the chief obstacles limiting the effect of cancer vaccines. Antigen-presenting cells (APCs) are primarily responsible for the induction of tumor-induced T-cell tolerance^{2,3}. We and others^{4,5} have identified a group of Gr-1⁺CD11b⁺ MDSCs that are primarily responsible for tumor-associated CD8⁺ T-cell tolerance. These are immature cells, comprising precursors of macrophages, granulocytes, dendritic cells (DCs) and myeloid cells at earlier stages of differentiation, and they have the ability to suppress immune response *in vitro* through direct cell–cell contact (reviewed in refs. 6–9). Accumulation of similar cells has been described in individuals with cancer^{10–12}. MDSCs induce antigen-specific MHC class I–restricted tolerance of CD8⁺ T cells *in vivo*⁴. This pathway may underlie antigen-specific inhibition of immune response in cancer and may explain the difficulties in maintaining the antigen-specific immune response after vaccination in individuals with cancer. The mechanism of MDSC-induced CD8⁺ T-cell tolerance, however, remains unclear.

There are two basic mechanisms of inducing T-cell tolerance: deletion and anergy. Existing data *in vitro* and *in vivo* indicate that MDSCs do not induce T-cell death or the deletion of antigen-specific T cells^{4–9}. Although much is known about the biochemical basis of T-cell anergy, the antigen-specific nature of T-cell tolerance is less understood^{13,14}. Using an experimental model *in vivo*, we show here that MDSCs, by generating reactive oxygen species (ROS) and peroxynitrite, induce modification of TCR and CD8 molecules, resulting in the loss of ability of CD8⁺ T cells to bind pMHC and the induction of antigen-specific non-responsiveness of peripheral CD8⁺ T cells. Our findings identify a previously unknown

mechanism of inducing T-cell tolerance in cancer and may be applicable to many pathological conditions (such as infection, inflammation, trauma) associated with the accumulation of MDSCs overproducing peroxynitrite.

RESULTS

MDSCs disrupt pMHC binding to CD8⁺ T cells

We used an experimental model in which the direct effect of MDSCs on antigen-specific CD8⁺ T cells could be evaluated *in vivo* (Supplementary Fig. 1 online). In this model, OT-1 T cells (CD45.1[−]) were transferred to naive CD45.1⁺ congenic recipients. MDSCs from EL-4 tumor-bearing mice were transferred 2 d later and mice were immunized with specific peptide. Lymph node cells were collected 10 d after immunization. By that time all transferred MDSCs either differentiated into mature myeloid cells or died (ref. 15 and data not shown) and did not directly interfere with any assay performed in lymph nodes. Donor CD45.1[−]CD8⁺ T cells from mice that received MDSCs had substantially lower ability to bind specific pMHC–Ig dimers than cells from control mice (Fig. 1a,b). A similar effect was observed in a different experimental system in which T cells from 2C transgenic mice were adoptively transferred to naive congenic mice and 2C-specific peptide was used for immunization (Supplementary Fig. 2a online). Repeated experiments showed that MDSC administration did not affect the expression of TCR or CD8 molecules on the surface of T cells (Fig. 1c and Supplementary Fig. 2).

Lymph node cells isolated from mice treated with MDSCs were re-stimulated *in vitro* with increasing concentrations of the specific peptides. The number of CD8⁺ T cells producing interferon-γ

¹H. Lee Moffitt Cancer Center, University of South Florida, 12902 Magnolia Drive, Tampa, Florida 33647, USA. ²John Hopkins University Medical School, 720 Rutland Avenue, Baltimore, Maryland 21205, USA. ³University of Nebraska Medical Center and Eppley Cancer Center, 986805 Nebraska Medical Center, Omaha, Nebraska 68198, USA. Correspondence should be addressed to D.I.G. (dmitry.gabrilovich@moffitt.org).

Received 20 July 2006; accepted 21 May 2007; published online 1 July 2007; doi:10.1038/nm1609

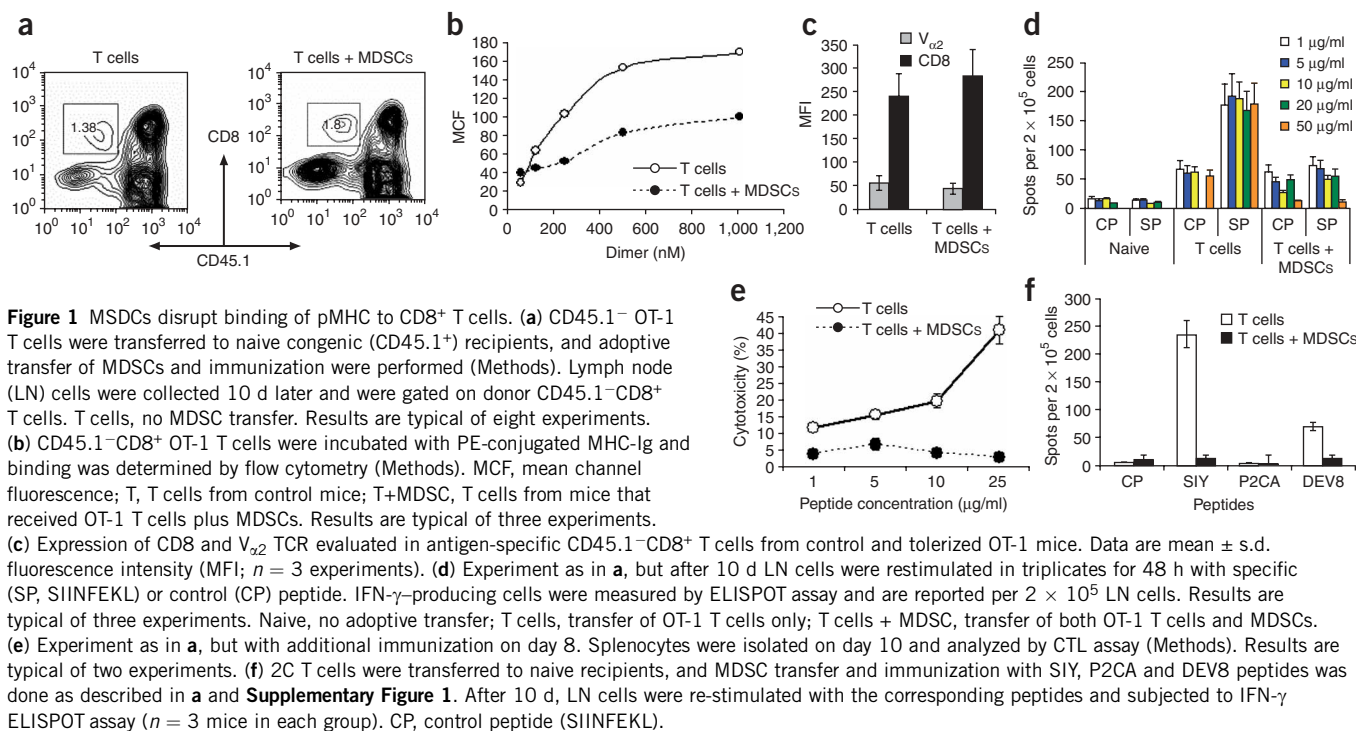


Figure 1 MSDCs disrupt binding of pMHC to CD8⁺ T cells. **(a)** CD45.1⁻ OT-1 T cells were transferred to naive congenic (CD45.1⁺) recipients, and adoptive transfer of MDSCs and immunization were performed (Methods). Lymph node (LN) cells were collected 10 d later and were gated on donor CD45.1⁻CD8⁺ T cells. T cells, no MDSC transfer. Results are typical of eight experiments. **(b)** CD45.1⁻CD8⁺ OT-1 T cells were incubated with PE-conjugated MHC-Ig and binding was determined by flow cytometry (Methods). MCF, mean channel fluorescence; T, T cells from control mice; T+MDSC, T cells from mice that received OT-1 T cells plus MDSCs. Results are typical of three experiments. **(c)** Expression of CD8 and V_{α2} TCR evaluated in antigen-specific CD45.1⁻CD8⁺ T cells from control and tolerized OT-1 mice. Data are mean ± s.d. fluorescence intensity (MFI; *n* = 3 experiments). **(d)** Experiment as in **a**, but after 10 d LN cells were restimulated in triplicates for 48 h with specific (SP, SIINFEKL) or control (CP) peptide. IFN- γ -producing cells were measured by ELISPOT assay and are reported per 2 × 10⁵ LN cells. Results are typical of three experiments. Naive, no adoptive transfer; T cells, transfer of OT-1 T cells only; T cells + MDSC, transfer of both OT-1 T cells and MDSCs. **(e)** Experiment as in **a**, but with additional immunization on day 8. Splenocytes were isolated on day 10 and analyzed by CTL assay (Methods). Results are typical of two experiments. **(f)** 2C T cells were transferred to naive recipients, and MDSC transfer and immunization with SIY, P2CA and DEV8 peptides was done as described in **a** and **Supplementary Figure 1**. After 10 d, LN cells were re-stimulated with the corresponding peptides and subjected to IFN- γ ELISPOT assay (*n* = 3 mice in each group). CP, control peptide (SIINFEKL).

(IFN- γ) was evaluated by ELISPOT assay. CD8⁺ T cells from MDSC-treated mice did not respond to the specific peptide. The response was not improved even by a 50-fold increase in peptide concentration (**Fig. 1d**). These data were confirmed in a cytotoxic T lymphocyte (CTL) assay against EL-4 and T2-K^b target cells. In both experimental models (OT-1 and 2C), T cells from control immunized mice showed peptide-specific CTL activity against target cells. By contrast, T cells from mice treated with MDSCs did not recognize specific targets. Increasing the concentration of the peptide used to load target cells did not improve CTL killing (**Fig. 1e** and **Supplementary Fig. 2c** online).

To address the possible role of TCR affinity in MDSC-mediated CD8⁺ T-cell tolerance, we used three peptides with different affinity to the 2C TCR: SIYRYGL (SIY) has high affinity, EQYKFYSV (DEV8) has intermediate affinity, and LSPFPFDL (P2CA) has low affinity^{16,17} SIY peptide induced a potent response of 2C CD8⁺ T cells and transfer

of MDSCs completely abolished this response (**Fig. 1f**). CD8⁺ T-cell response to DEV8 peptide was much weaker. It also was blocked by MDSCs. No response was detected against P2CA peptide.

Mechanism of disruption of pMHC binding to CD8⁺ T cells

Previous studies have shown that MDSCs produce large amounts of ROS⁸. To clarify the role of ROS in MDSC-induced T-cell tolerance *in vivo*, we used mice lacking gp91^{phox}, an essential component of the NADPH complex (ref. 18). MDSCs from mice genetically deficient in gp91^{phox} (encoded by gp91^{phox}, also known as *Cybb*) have little or no ROS but maintain MHC class I expression (data not shown). In contrast to MDSCs from wild-type tumor-bearing mice, MDSCs isolated from gp91^{phox}^{-/-} tumor-bearing mice did not induce CD8⁺ T-cell tolerance (**Fig. 2a**).

After interaction with nitric oxide (NO), O₂⁻ forms peroxynitrite (ONOO⁻) with a high biological activity¹⁹. MDSCs produce large

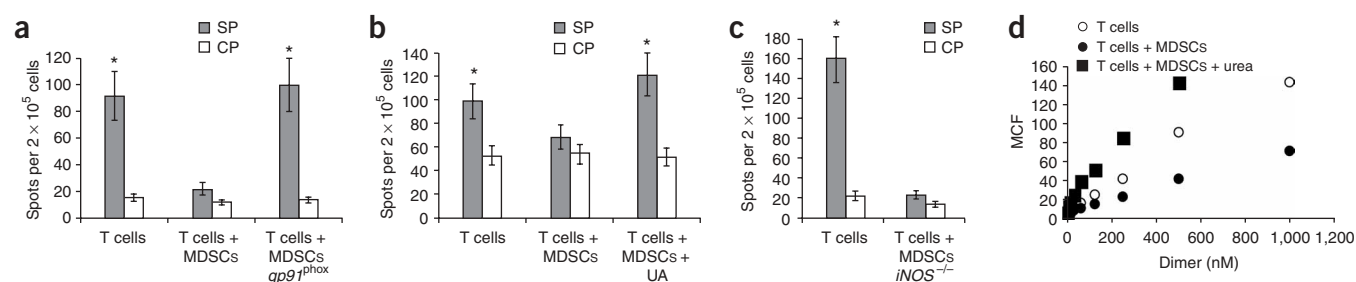


Figure 2 Mechanism of MDSC-induced T-cell tolerance. Adoptive transfer and immunization was done as described in **Figure 1**. **(a–c)** IFN- γ ELISPOT assay of lymph node (LN) cells re-stimulated with control (CP) or specific (SP) peptides. Results are mean ± s.d. per 2 × 10⁵ LN cells. **P* < 0.05 between CP and SP groups (paired *t*-test). **(a)** MDSCs from EL-4 tumor-bearing gp91^{phox}^{-/-} or wild-type mice were used for adoptive transfer (*n* = 3 experiments). **(b)** Mice were treated with uric acid in suspension (20 mg in 100 μ l) on days -1, 0, 1 and 2 after MDSC transfer. **(c)** MDSCs from EL-4 tumor-bearing *iNOS*^{-/-} mice were used for adoptive transfer. Results are typical of two experiments. **(d)** LN cells from OT-1 mice were cultured with 10 μ g/ml of SIINFEKL and MDSCs (3:1 ratio) for 48 h in 1 mg/ml of urea. Binding of control and specific pMHC to CD8⁺ T cells was evaluated by flow cytometry as described in **Figure 1**. T, T cells incubated alone; T + MDSC, T cells incubated with MDSCs; T + MDSC + urea, T cells incubated with MDSCs and urea.

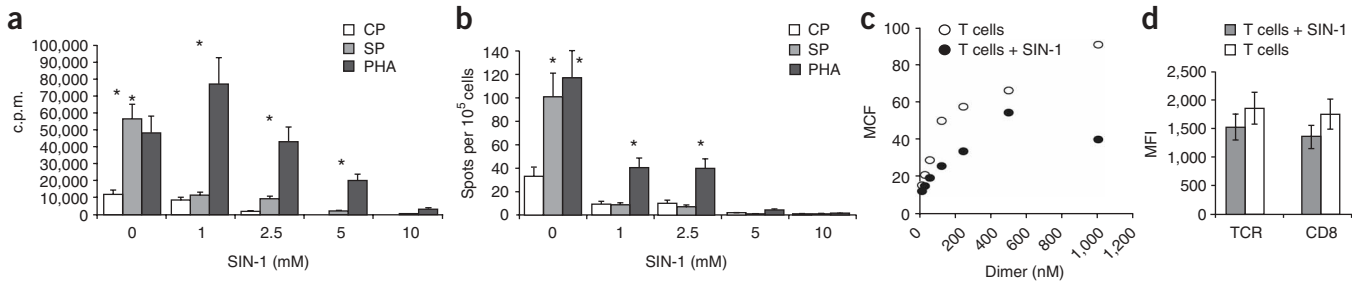


Figure 3 Effect of peroxynitrite donor on specific CD8⁺ T-cell activity. **(a)** OT-1 T cells were pretreated with SIN-1 for 30 min, and then 5×10^4 T cells were cultured for 4 d with DCs loaded with 10 $\mu\text{g}/\text{ml}$ of either control peptide (CP, RAHYNIVTF) or specific peptide (SP, SIINFEKL) at a 10:1 ratio. PHA, OT-1 T cells and DCs cultured for 3 d in the presence of 1 $\mu\text{g}/\text{ml}$ of PHA³. [³H]Thymidine (1 $\mu\text{Ci}/\text{well}$) was added 18 h before cells were collected, and radioactivity was measured in triplicates in a liquid scintillation counter. **(b)** OT-1 T cells were cultured for 48 h with DCs, peptide and PHA as described in **a**. IFN- γ -producing cells were measured in quadruplicates by ELISPOT assay. **(c)** OT-1 T cells were pretreated with 1 mM SIN-1 for 30 min. Binding of control and specific pMHC dimers to CD8⁺ T cells was evaluated by flow cytometry as described in **Figure 1**. T, T cells stimulated with specific peptide-loaded DCs; T+Sin-1, T cells pretreated with SIN-1. **(d)** Cells were treated as described in **c** and then labeled with antibody to CD8, TCR- α or TCR- β . Expression within the population of CD8⁺ T cells was evaluated by flow cytometry ($n = 3$ experiments). Data are mean \pm s.d. (**a–d**).

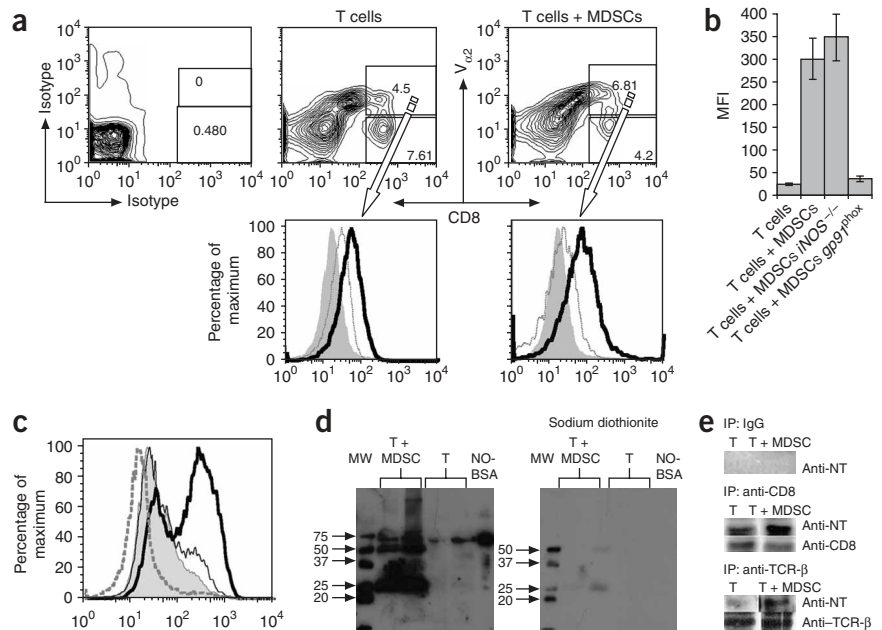
amounts of peroxynitrite²⁰. To evaluate the possible role of ONOO⁻ in MDSC-mediated T-cell tolerance, mice that had undergone adoptive transfer of OT-1 T cells and MDSCs were treated with uric acid, a compound that specifically neutralizes peroxynitrite^{21,22}. Uric acid completely abrogated the tolerogenic effect of MDSCs (**Fig. 2b**). A previous study has described the ability of uric acid in crystal form to activate APCs²³, whereas we used a soluble form of uric acid. To evaluate directly the possible effect of uric acid on APC activation, mice were treated for 48 h with the acid, and the phenotype and function of DCs were evaluated. No differences between control and treated mice were found (data not shown).

In contrast to activated macrophages, MDSCs often do not show significant upregulation of nitric oxide^{20,24}. To elucidate the role of nitric oxide in MDSC-mediated T-cell tolerance, we used mice genetically deficient in inducible nitric oxide synthase (iNOS, encoded

by *iNOS*, also known as *Nos2*). These mice cannot upregulate nitric oxide production in response to different stimuli; however, they retain basal nitric oxide production because of the activity of other NOS, primarily endothelial NOS (eNOS)²⁵. MDSCs from *iNOS*^{-/-} tumor-bearing mice had the same ability to induce CD8⁺ T-cell tolerance as MDSCs from wild-type tumor-bearing mice (**Fig. 2c**). These data indicated that upregulation of ROS but not nitric oxide was primarily responsible for MDSC-mediated CD8⁺ T-cell tolerance. Neutralization of peroxynitrite with urea completely abrogated MDSC-mediated decrease in the binding of the specific pMHC to CD8⁺ T cells *in vitro* (**Fig. 2d**), suggesting that peroxynitrite has a critical role in the disruption of pMHC binding to CD8⁺ T cells.

To verify the possible role of peroxynitrite in CD8⁺ T cell tolerance, we used a donor of peroxynitrite, 3-morpholinosydnonimine (SIN-1). OT-1 T cells were pre-treated for 30 min with different concentrations

Figure 4 Role of MDSCs in the nitration of tyrosine in CD8⁺ T cells. **(a)** Adoptive transfer and immunization were done as described in **Figure 1** and **Supplementary Figure 1**. After 8 d, lymph nodes were isolated and labeled with antibodies to CD8, V α 2 and nitrotyrosine (NT). Expression of NT was evaluated in donor (CD8⁺V α 2⁺; thick line) and recipient (CD8⁺V α 2⁻; thin line) populations. Shaded areas show isotype control IgG. **(b)** Splenocytes from OT-1 mice were cultured for 72 h with control or specific peptides and MDSCs (3:1 ratio) from wild-type, *gp91^{phox}-/-* or *iNOS*^{-/-} EL-4 tumor-bearing mice. Expression of NT in CD8⁺ T cells was evaluated by flow cytometry. Data are mean \pm s.d. ($n = 3$ experiments). **(c)** Expression of NT in CD8⁺ OT-1 T cells. Cells were treated as in **b**. Shaded area, splenocytes alone; thick line, splenocytes plus MDSCs; broken line, +1 mM SOD; thin line, +1 mM L-NMMA. Cells were gated on CD8 and NT expression was measured. MFI of samples with control peptides was <30 in all experiments in **c,d** (not shown). **(d)** Splenocytes from OT-1 mice were cultured for 48 h with specific peptide and MDSCs (3:1 ratio). Whole-cell lysates were subjected to immunoblotting for NT (Methods). Each experiment was done in duplicate. **(e)** Splenocytes cells from OT-1 mice were treated as in **d** and subjected to immunoprecipitation with antibody to CD8 or TCR- β (Methods). Rabbit IgG was used in control experiments. To verify loading, the same blots were stripped and re-probed with antibody to CD8 or TCR- β .



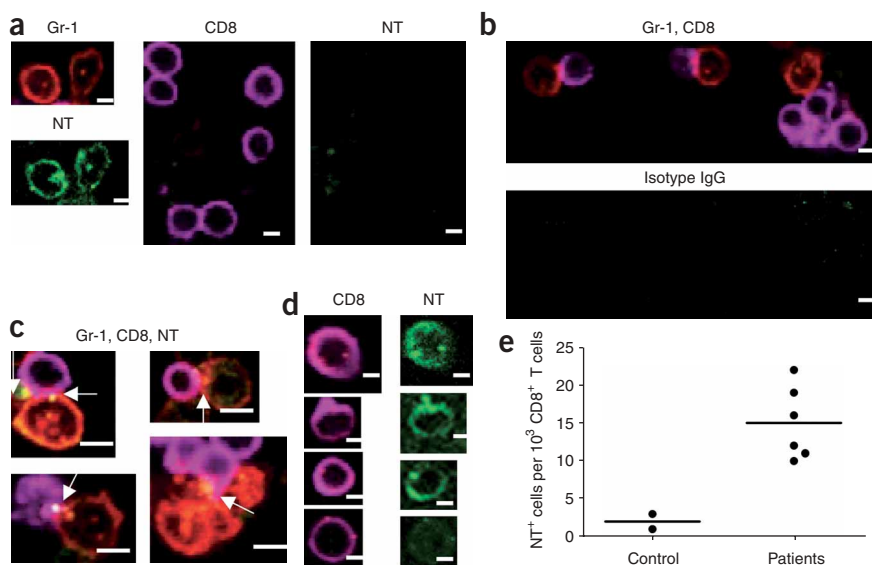


Figure 5 Interaction between MDSCs and CD8⁺ T cells. (a–d) Splenocytes from OT-1 mice were cultured with specific peptide and MDSCs (3:1 ratio). Cells were labeled with anti-Gr-1-PE (red), anti-CD8-Alexa 647 (magenta), anti-nitrotyrosine-Alexa 488 (green) or isotype-Alexa 488 (green) at different time points and visualized by confocal microscopy. (a) MDSCs and CD8⁺ T cells separated before co-culture. (b,c) Staining after 5 h of co-culture. Arrows denote nitrotyrosine (NT) localized at contacts between MDSCs and CD8⁺ T cells. (d) Staining after 48 h of co-culture. (e) Number of NT-positive cells per 10³ CD8⁺ T cells in lymph nodes from individuals with breast or head and neck cancers. Lymph nodes without tumors were further evaluated (see **Supplementary Fig. 5**). Scale bar, 10 μ m.

of SIN-1 and then stimulated with either peptide-pulsed DCs or phytohemagglutinin (PHA). At 1 mM, SIN-1 did not affect cell viability (data not shown) but completely abrogated peptide-specific CD8⁺ T-cell proliferation and IFN- γ production (**Fig. 3a,b**) and it substantially reduced specific pMHC binding to CD8⁺ T cells (**Fig. 3c**) but did not affect the expression of TCR or CD8 on the T cell surface (**Fig. 3d**). PHA-inducible T-cell proliferation was not affected (**Fig. 3a**), whereas IFN- γ production was reduced, although it remained substantially higher than in the control (**Fig. 3b**). A higher dose of SIN-1 resulted in a progressive decrease in cell viability (data not shown) and T-cell proliferation (**Fig. 3a**) and complete abrogation of IFN- γ production (**Fig. 3b**). These data show that, at a relatively low dose, SIN-1 reduces the pMHC binding and blocks peptide-specific responses, but has a limited effect on nonspecific stimulation of CD8⁺ T cells. This effect is similar to that exerted by MDSCs *in vivo*.

Role of nitration of TCR complex in CD8⁺ T-cell tolerance

The main effect of peroxynitrite is its ability to modify proteins through oxidation or nitration of different amino acids. One of the main targets of peroxynitrite activity is tyrosine, which creates nitrotyrosine. Nitration of tyrosine is relatively stable²⁶ and has been shown to impede the function of the proteins through alteration of the hydrogen-bond, van der Waals and electrostatic network²⁷. We considered that nitration of tyrosine in the pMHC-TCR complex might increase its rigidity and disable its integrity. Molecular modeling of the 2C TCR indicated that nitration of tyrosine at several sites in TCR and CD8 would markedly alter recognition of pMHC (**Supplementary Figs. 3 and 4** online).

We tested whether MDSCs could cause nitration of TCR-CD8 in antigen-specific CD8⁺ T cells. Lymph node cells were isolated from mice after adoptive transfer of OT-1 T cells and MDSCs, and immunization. With gating on donor peptide-specific CD8⁺V₂₂⁺ T cells and recipient CD8⁺V₂₂⁻ T cells, nitrotyrosine on the cell surface was evaluated with a nitrotyrosine-specific antibody (**Fig. 4a**). CD8⁺V₂₂⁺ and CD8⁺V₂₂⁻ cells from control immunized mice showed similar expression of nitrotyrosine. By contrast, CD8⁺V₂₂⁺ cells from MDSC recipients had much more nitrotyrosine (**Fig. 4a**). OT-1 CD8⁺ T cells were pre-activated with specific peptide for 72 h and then incubated for 48 h with MDSCs isolated from tumor-bearing mice. MDSCs substantially increased nitrotyrosine in OT-1 CD8⁺ cells

(**Fig. 4b,c**). MDSCs isolated from *gp91^{phox}-/-* but not *iNOS^{-/-}* mice did not induce nitrotyrosine expression on the T-cell surface (**Fig. 4b**). Treatment of MDSCs with the ROS inhibitor sodium dismutase (SOD) and the NOS inhibitor L-NMMA blocked the MDSC-inducible increase in nitrotyrosine (**Fig. 4c**). L-NMMA inhibits the activity of both eNOS and iNOS, and thus reduces basal NO production²⁸, which may explain the difference between these results and those obtained with *iNOS^{-/-}* MDSCs.

We incubated activated OT-1 T cells with MDSCs for 48 h in the presence of specific peptide. T cells were isolated and whole-cell lysates were analyzed by immunoblotting with a nitrotyrosine-specific antibody. Treatment of T cells with MDSCs resulted in several bands positive for nitrotyrosine (**Fig. 4d**). Treatment of the membranes with sodium dithionite, which causes chemical reduction of nitrotyrosine to aminotyrosine, completely eliminated binding (**Fig. 4d**), indicating that bands detected indeed contained nitrotyrosine. We tested whether TCR and CD8 molecules could be the targets for MDSC-mediated nitration. Proteins were precipitated with antibody to TCR- β , CD8 or control IgG, subjected to electrophoresis, and then probed with a nitrotyrosine-specific antibody. MDSCs induced a substantial increase in nitrotyrosine in both TCR- β and CD8 (**Fig. 4e**).

Interaction between MDSCs and CD8⁺ OT-1 T cells in the presence of specific peptide was evaluated by confocal microscopy. Almost all Gr-1⁺ MDSCs were positive for nitrotyrosine localized both on the membrane and in cytoplasm (**Fig. 5a**). CD8⁺ T cells were negative for nitrotyrosine. After 5 h of incubation, direct contacts between Gr-1⁺ MDSCs and CD8⁺ OT-1 T cells were readily detectable (**Fig. 5b**). Nitrotyrosine in CD8⁺ T cells was primarily localized on the membrane at the point of interaction between MDSCs and CD8⁺ T cells (**Fig. 5c**). After 48 h incubation with MDSCs, diffuse membrane nitrotyrosine staining of CD8⁺ T cells was evident (**Fig. 5d**).

We tested whether nitrotyrosine-positive CD8⁺ T cells could be found in lymph nodes from tumor-bearing hosts. We studied lymph nodes obtained from six individuals with breast or head and neck cancer. Only lymph nodes free of tumor cells were evaluated. As a control, lymphoid tissues (tonsils) from two tumor-free individuals were used. Very few nitrotyrosine-positive CD8⁺ T cells were found in control samples, whereas lymph nodes from individuals with cancer contained detectable nitrotyrosine-positive CD8⁺ T cells (**Fig. 5e** and **Supplementary Fig. 5** online).

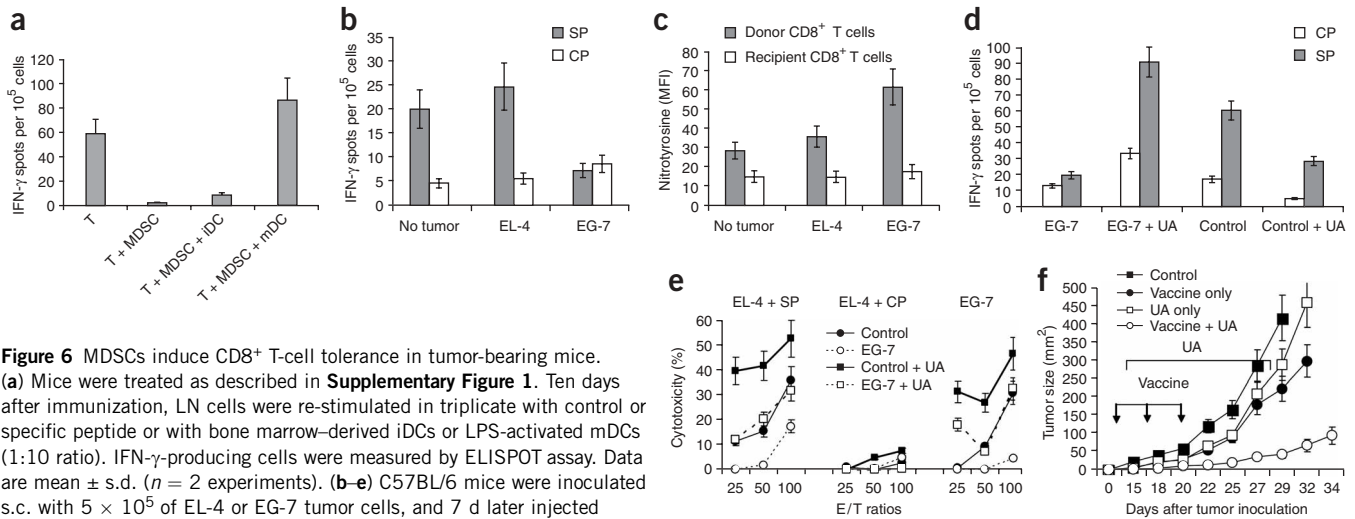


Figure 6 MDSCs induce CD8⁺ T-cell tolerance in tumor-bearing mice.

(a) Mice were treated as described in **Supplementary Figure 1**. Ten days after immunization, LN cells were re-stimulated in triplicate with control or specific peptide or with bone marrow-derived iDCs or LPS-activated mDCs (1:10 ratio). IFN- γ -producing cells were measured by ELISPOT assay. Data are mean \pm s.d. ($n = 2$ experiments). (b–e) C57BL/6 mice were inoculated s.c. with 5×10^5 of EL-4 or EG-7 tumor cells, and 7 d later injected i.v. with 5×10^6 OT-1 T cells. After a further 7 d, mice were killed.

(b) LN cells were stimulated with specific (SP, SIINFEKL) or control (CP, RAHYNIVTF) peptides and analyzed by IFN- γ ELISPOT assay. Data are reported per 10^5 LN cells ($n = 3$ mice per group). Differences between SP and CP were significant for both control and EL-4 tumor-bearing mice ($P < 0.05$, paired t -test). (c) Splenocytes were labeled with antibody to CD8, V α 2 or nitrotyrosine (NT). Expression of NT was evaluated in donor (CD8⁺V α 2⁺) and recipient (CD8⁺V α 2⁻) cells. Data are mean \pm s.d. ($n = 2$ experiments). Differences between NT in donor cells from EG-7 mice and EL-4 or control mice were statistically significant ($P < 0.05$ in paired t -test). (d) EG-7 tumor-bearing mice were treated with uric acid (Methods). LN cells were analyzed 7 d later. (e) Splenocytes from EG-7 tumor-bearing mice were used as effectors in a CTL assay (Methods). Each experiment was performed in duplicate ($n = 3$ mice per group). Data are mean \pm s.d. (f) MC38 tumors were established in C57BL/6 mice. Mice in the treatment group (vaccine plus uric acid) were injected with DC-Ad-p53 vaccine as described²⁹. Immunizations were repeated twice at 5–6-d interval. Treatment with uric acid (20 mg/100 μ l PBS) was started 2 d after the first immunization and continued for 2 weeks. Data are mean \pm s.d. ($n = 5$ –6 mice per group).

Reversal of MDSC-induced CD8⁺ T-cell tolerance

MDSC-induced CD8⁺ T-cell tolerance persisted for at least 3 weeks. The response in control mice gradually decreased with time (**Supplementary Fig. 6a,b** online); however, 22 d after immunization the peptide-specific response was still detectable in lymph nodes of control, but not MDSC-treated, mice (**Supplementary Fig. 6b**). Stimulation with peptide-loaded lipopolysaccharide (LPS)-activated mature DCs (mDCs) but not immature DCs (iDCs) overcame MDSC-induced T-cell tolerance (**Fig. 6a**).

We examined whether CD8⁺ T-cell tolerance could be observed in tumor-bearing mice. These mice would have ‘natural’ tumor-associated antigens and MDSCs. We provided only the source of antigen-specific T-cells. Two types of tumor were used: EL-4 cells expressing ovalbumin (EG-7) and parental EL-4 tumors. We previously determined that both EL-4 and EG-7 tumors result in an accumulation of MDSCs, which can process and present OVA-derived epitope on their surface⁴. OT-1 T-cells were transferred to EL-4 and EG-7 tumor-bearing mice, and mice were killed 7 d later. Lymph nodes from control mice contained very few Gr-1⁺ cells, whereas lymph nodes from tumor-bearing mice were packed with these cells (**Supplementary Fig. 7a,b** online) located in T-cell areas in direct contact with CD8⁺ T cells (**Supplementary Fig. 7c**). Lymph node cells were stimulated with specific or control peptides and the responses were evaluated by IFN- γ ELISPOT assay. Control tumor-free mice demonstrated a low (because T cells were not activated *in vivo*) but clearly detectable specific response. A similar response was found in EL-4 tumor-bearing mice. By contrast, no specific response was observed in lymph nodes from EG-7 tumor-bearing mice (**Fig. 6b**). The amount of nitrotyrosine in recipient V α 2⁺CD8⁺ T cells was similar in all groups of mice. It was, however, considerably higher in donor V α 2⁺CD8⁺ T cells from EG-7 tumor-bearing mice than in those from control or EL-4 tumor-bearing mice (**Fig. 6c**).

To identify the potential role of peroxynitrite in this process, EG-7 tumor-bearing mice were treated with daily intraperitoneal (i.p.)

injections of uric acid starting from the day of adoptive transfer of OT-1 T cells. After 7 d, lymph node cells were isolated and re-stimulated with control or specific peptides. In tumor-bearing mice, OT-1 CD8⁺ T cells lost the ability to respond to stimulation with specific peptide, as assessed by IFN- γ ELISPOT (**Fig. 6d**) and CTL (**Fig. 6e**) assays. Treatment with uric acid completely prevented the development of T-cell tolerance (**Fig. 6d,e**). To eliminate the possibility that uric acid can induce nonspecific T-cell activation, naive C57BL/6 mice were treated with daily uric acid i.p. injections for 7 d. Spleen and lymph node T cells were analyzed for the expression of CD25 and CD69 molecules and for proliferation in response to different stimuli. Treatment with uric acid did not result in activation of T cells (**Supplementary Fig. 8** online).

We addressed the possibility that blocking peroxynitrite may improve the anti-tumor effect of a cancer vaccine in a non-transgenic experimental system. An MC38 tumor was established in C57BL/6 mice by subcutaneous (s.c.) injection of tumor cells. On day 10 after tumor inoculation, when tumors were palpable, mice were split into four groups with equal tumor size. Mice in the treatment group were immunized with DC-Ad-p53 vaccine as described²⁹. Treatment with uric acid was started 3 d after the first immunization and was continued for 2 weeks. Control groups included mice treated with uric acid alone or vaccine alone, and untreated mice. Immunization of mice with established tumors resulted only in a temporal delay of tumor growth, which resumed 7 d after treatment had finished. Uric acid alone only marginally delayed tumor growth. By contrast, a combination of vaccination with uric acid resulted in a substantial delay in tumor growth (**Fig. 6f**).

DISCUSSION

MDSCs are produced in response to various tumor-derived cytokines and represent a mixed population of myeloid cells at different stages of differentiation^{7,10,30–32}. In addition to cancer,

many pathological conditions including traumatic stress, bacterial and parasitic infections have been reported to have increased production of MDSCs^{33–35}. Studies from several groups have implicated MDSCs in tumor-associated T-cell tolerance^{4,5}. To understand the mechanism of this process, we have used an experimental model based on adoptive transfer of T cells and MDSCs into naive congenic recipients. Tumor-free recipients enabled us to avoid the various confounding effects of tumor. In both experimental systems tested, MDSCs induced a marked decrease in the binding of specific pMHC to CD8⁺ T cells. Although this effect has not been described in cancer, it is known that the changes in TCR binding avidity can be important in regulating antigen sensitivity^{36–38} (see **Supplementary Discussion** online).

Our experiments showed that ROS have a crucial role in MDSC-mediated T-cell tolerance. ROS can modify proteins directly or in combination with nitric oxide, contributing to generation of peroxynitrite. Here, a peroxynitrite scavenger completely eliminated MDSC-induced T-cell tolerance. Nitration of tyrosine has long been recognized as a marker of peroxynitrite activity. Peroxynitrite-dependent tyrosine nitration is likely to occur through the initial reaction of peroxynitrite with carbon dioxide or metal centers, leading to secondary nitrating species as nitrogen dioxide radicals³⁹. In addition, peroxynitrite can react directly with cysteine, methionine and tryptophan³⁹. It is likely that tyrosine nitration represents only part of the total peroxynitrite activity in this experimental system.

Molecular modeling identified many tyrosine residues in TCR and CD8 that could be susceptible to nitration, and structural analysis showed that nitration of these residues would result in decreased flexibility and increased rigidity of TCR domains, which might significantly alter the epitope-specific interactions between TCR and pMHC. Our observation of substantially more nitrotyrosine on the surface of antigen-specific CD8⁺ T cells from mice treated with MDSCs confirmed the antigenic specificity of the tolerance induced by contacts with MDSCs.

These results suggest a previously unknown mechanism of CD8⁺ T-cell tolerance in cancer and possibly in other pathological conditions associated with MDSC accumulation. MDSCs that accumulate in tumor-bearing hosts contain large amounts of ROS and peroxynitrite. Because these substances are short-lived and highly reactive, they are active only at very short distances. The interface between MDSCs and CD8⁺ T cells interacting during antigen-TCR recognition provides such an environment. The amount of peroxynitrite produced by MDSCs is sufficient to nitrate tyrosine exposed on the surface of contacting cells. Modified tyrosine on TCR and CD8 alters the conformational flexibility of TCR chains, leading to loss of the response to specific antigen. We suggest that a similar process of tumor-induced peripheral immunological tolerance may potentially operate by using other post-translational modifications of proteins in the TCR-pMHC complex. Such a mechanism may explain the well-established fact that tumor-bearing hosts do not have profound systemic immune deficiency and T cells retain their ability to respond to other stimuli, including viruses, lectins and interleukin 2 (IL-2), among others. Our study provides additional support to the theory of preventing the nitrotyrosine formation in cancer immunotherapy⁴⁰. Blocking peroxynitrite generation or using scavengers could represent an attractive opportunity to decrease or even to eliminate MDSC-induced T-cell tolerance and to enhance the effect of cancer immunotherapy. More potential molecular targets may be discovered if other tumor-induced post-translational modifications of proteins involved in T cell-APC interactions are explored.

METHODS

Mice and reagents. All mouse experiments were approved by the University of South Florida Institutional Animal Care and Use Committee. Female C57BL/6 mice (aged 6–8 weeks) were obtained from the National Cancer Institute. We purchased OT-1 TCR-transgenic mice (C57BL/6-Tg(TCR α TCR β)1100mjb), *gp91^{phox}-/-* (B6.129S6-Cybb^{tm1Din}), *iNOS^{-/-}* (C57BL6-Nos2^{tm1Lau}) and CD45.1⁺ congenic mice (B6.SJL-PtrcaPep3b/BoyJ) from Jackson Laboratories. 2C TCR transgenic mice have been described⁴¹. To establish EL-4 and EG-7 tumors, C57BL/6 mice were injected s.c. with 5×10^5 EL-4 or EG-7 cells, respectively. MC38 tumors were established in C57BL/6 mice by s.c. injection of 3.5×10^5 tumor cells. Tumor size was measured with calipers and is presented as the multiplication of the two longest dimensions. Some EG-7 tumor-bearing mice were treated with daily i.p. injections of uric acid (20 mg in 100 μ l of PBS) starting on the day of adoptive transfer of OT-1 cells.

OVA-derived (H-2K^b, SIINFEKL), 2C-specific (H-2K^b SIY and H-2L^d QLSPPFDL) and control (H-2K^b RAHYNIVTF) peptides were obtained from QCB. Incomplete Freund's adjuvant (IFA) and uric acid were purchased from Sigma. We obtained all antibodies used for flow cytometry from BD Pharmingen except anti-nitrotyrosine (Upstate USA Inc.).

Cell isolation and generation. Gr-1⁺ cells were isolated from spleens of tumor-bearing mice by using magnetic beads and MiniMACS columns (Miltenyi Biotec) and biotinylated antibody to Gr-1. More than 98% of Gr-1⁺ cells were also CD11b⁺ (**Supplementary Fig. 1**). We isolated T lymphocytes from spleens by using T-cell enrichment columns (R&D Systems), and generated DCs from murine bone marrow using granulocyte-macrophage colony-stimulating factor (Invitrogen) and interleukin-4 (IL-4; R&D Systems) as described⁴². DCs were activated on day 6 of culture by overnight incubation with LPS (1 μ g/ml). On day 7, cells were collected and DCs were enriched by centrifugation over Nycoprep A gradient (Accurate Chemicals). To pulse DCs with peptide, cells were washed in PBS and incubated with either specific or control peptide (10 μ g/ml) at 37 °C for 2 h.

Adoptive cell transfer and immunization. Naive C57BL/6 recipient mice were injected intravenously (i.v.) with $4\text{--}5 \times 10^6$ purified T cells from OT-1 or 2C TCR transgenic mice. After 2–3 d, the mice were injected i.v. with $4\text{--}5 \times 10^6$ MDSCs and within an hour immunized s.c. with 100 μ g of specific peptide in IFA. After 10 d, cells from lymph nodes were re-stimulated with specific or control peptide and analyzed (**Supplementary Fig. 1**).

ELISPOT. We evaluated the number of IFN- γ -producing cells in response to stimulation to specific or control peptide (10 μ g/ml) by ELISPOT assay as described⁴³. Each well contained 2×10^5 lymph nodes cells. The number of spots were counted in triplicates and calculated by an automatic ELISPOT counter (Cellular Technology).

Antigen-binding assay. Fluorescently labeled H2-K^b-Ig dimers were prepared as described³⁶, cells were incubated with various amounts of dimer (1.20×10^{-6} to 6.25×10^{-8} M), and dimer binding to T cells was measured by flow cytometry using a FACScalibur (Becton Dickinson). Specific binding of the dimer was calculated by subtracting nonspecific binding (measured using K^b-Ig loaded with irrelevant peptide) from the total binding.

CTL assay. Splenocytes were tested in a standard 6-h ⁵¹Cr-release CTL assay. In **Figure 1e**, the target cells were EL-4 cells loaded with specific or control peptides at the indicated concentrations. Cells were incubated in duplicates at a 25:1 effector/target ratio. The level of nonspecific cytotoxicity (EL-4 target cells loaded with control peptide) was subtracted. Background cytotoxicity was less than 10%. In **Figure 6e**, splenocytes from EG-7 tumor-bearing mice were stimulated *ex vivo* for 7 d with SIINFEKL peptide (10 μ g/ml), in the presence of IL-15 (10 ng/ml) and IL-21 (10 ng/ml) and used as effectors in a standard 6-h ⁵¹Cr-release CTL assay. Target cells were either EL-4 cells pulsed with 10 μ g/ml of either specific (SIINFEKL) or control (RAHYNIVTF) peptides, or EG7 cells. Different effector/target cell ratios were used.

Immunoblotting and immunoprecipitation. T cells were collected, washed in PBS and lysed. Whole-cell lysates were subjected to 10% SDS-PAGE, transferred to PVDF membrane and probed with antibody to nitrotyrosine. Nitrated BSA

(NO-BSA) was used as a positive control for nitrotyrosine staining. Bands were visualized by electrochemiluminescence. Chemical reduction of nitrotyrosine was done using sodium dithionite. In some experiments, antibody to CD8 or TCR- β was added to whole-cell lysates (500 μ g of protein per sample) and incubated for 2 h at 4 °C. Protein A–Sepharose beads (eBioscience) were then added, and after 1 h the mixture was washed, re-suspended in Laemmli SDS sample buffer and denatured at 95 °C for 5 min. Samples were resolved by 10% SDS-PAGE, transferred to PVDF membrane and probed with antibody to nitrotyrosine, CD8 and TCR- β .

Molecular modeling of TCR–H-2K^b–peptide complex. We used the Biopolymer module of the SYBYL 7-1 software package (Tripos) to analyze structural effects of TCR nitration on interactions in the pMHC–TCR complex. Crystal structures of the TCR–H-2K^b–SIY and TCR–H-2K^b–DEV8 complexes (PDB codes: 1G6R, 2CKB and 1MWA) were used as templates for modeling and analysis of intermolecular interactions for both native and nitrated pMHC–TCR complexes. After adding all hydrogen atoms to the crystal structures, the molecular structures were energy-minimized by using the MMFF94s force field implemented in SYBYL. Energy minimizations were performed by 300 cycles of conjugate gradient minimization, and potential hydrogen bonds were visualized and analyzed with Biopolymer.

Confocal microscopy. Splenocytes from OT-1 mice were cultured with specific peptide in the presence of MDSCs (3:1 ratio) on a poly-D-lysine-coated glass-bottom culture dish (MatTek). We labeled the cells with anti-Gr-1-PE, anti-CD8–Alexa 647, anti-nitrotyrosine–Alexa 488 or isotype IgG–Alexa 488. Cells were viewed with a DMI6000 inverted Leica TCS AOBs SP5 tandem scanning confocal microscope with a 40 \times , 1.30 NA oil immersion objective. Tunable 488-nm argon and 546-nm and 633-nm laser lines were applied to excite the samples by using AOBs line switching to minimize crosstalk between fluorochromes. Images and z-stacks were produced with three cooled photomultiplier detectors and the LAS AF version 1.5.1.889 software suite.

Note: Supplementary information is available on the Nature Medicine website.

ACKNOWLEDGMENTS

We thank S. Kusmartsev for assistance at the beginning of this project and J. DeComarmond for technical assistance with manuscript preparation. This work was supported by the National Institutes of Health (grant RO1CA 84488 to D.I.G.) and, in part, by the Analytic Microscopy and Flow Cytometry Core Facility at the H. Lee Moffitt Cancer Center.

AUTHOR CONTRIBUTIONS

S.N. performed most of the experiments, analyzed data and wrote the manuscript; K.G. performed some of binding experiments; V.P. contributed to overall research design and molecular modeling analysis; L.K. performed molecular modeling analysis; S.S. performed molecular modeling analysis; L.K. performed immunohistology in human tissues; D.H. performed immunohistology in mouse tissues; J.S. contributed to overall research design and analysis; D.I.G. designed the experiments, analyzed the data, wrote the manuscript and supervised the project.

COMPETING INTERESTS STATEMENT

The authors declare no competing financial interests.

Published online at <http://www.nature.com/naturemedicine/>

Reprints and permissions information is available online at <http://npg.nature.com/reprintsandpermissions>

- Pardoll, D. Does the immune system see tumors as foreign or self? *Annu. Rev. Immunol.* **21**, 807–839 (2003).
- Sotomayor, E.M. *et al.* Conversion of tumor-specific CD4⁺ T-cell tolerance to T-cell priming through *in vivo* ligation of CD40. *Nat. Med.* **5**, 780–787 (1999).
- Cuenca, A. *et al.* Extra-lymphatic solid tumor growth is not immunologically ignored and results in early induction of antigen-specific T-cell anergy: dominant role of cross-tolerance to tumor antigens. *Cancer Res.* **63**, 9007–9015 (2003).
- Kusmartsev, S., Nagaraj, S. & Gabrilovich, D.I. Tumor-associated CD8⁺ T cell tolerance induced by bone marrow-derived immature myeloid cells. *J. Immunol.* **175**, 4583–4592 (2005).
- Huang, B. *et al.* Gr-1⁺CD115⁺ immature myeloid suppressor cells mediate the development of tumor-induced T regulatory cells and T-cell anergy in tumor-bearing host. *Cancer Res.* **66**, 1123–1131 (2006).

- Serafini, P., Borrello, I. & Bronte, V. Myeloid suppressor cells in cancer: recruitment, phenotype, properties, and mechanisms of immune suppression. *Semin. Cancer Biol.* **16**, 53–65 (2006).
- Gabrilovich, D. The mechanisms and functional significance of tumour-induced dendritic-cell defects. *Nat. Rev. Immunol.* **4**, 941–952 (2004).
- Kusmartsev, S. & Gabrilovich, D.I. Role of immature myeloid cells in mechanisms of immune evasion in cancer. *Cancer Immunol. Immunother.* **55**, 237–245 (2006).
- Sinha, P., Clements, V.K., Miller, S. & Ostrand-Rosenberg, S. Tumor immunity: a balancing act between T cell activation, macrophage activation and tumor-induced immune suppression. *Cancer Immunol. Immunother.* **54**, 1137–1142 (2005).
- Almand, B. *et al.* Increased production of immature myeloid cells in cancer patients. A mechanism of immunosuppression in cancer. *J. Immunol.* **166**, 678–689 (2001).
- Schmielau, J. & Finn, O.J. Activated granulocytes and granulocyte-derived hydrogen peroxide are the underlying mechanism of suppression of T-cell function in advanced cancer patients. *Cancer Res.* **61**, 4756–4760 (2001).
- Zea, A.H. *et al.* Arginase-producing myeloid suppressor cells in renal cell carcinoma patients: a mechanism of tumor evasion. *Cancer Res.* **65**, 3044–3048 (2005).
- Appleman, L.J., Tzachanis, D., Grader-Beck, T., van Puijnenbroek, A.A. & Boussiotis, V.A. Helper T cell anergy: from biochemistry to cancer pathophysiology and therapeutics. *J. Mol. Med.* **78**, 673–683 (2001).
- Steinman, R.M. & Nussenzweig, M.C. Avoiding horror autotoxicus: the importance of dendritic cells in peripheral T cell tolerance. *Proc. Natl. Acad. Sci. USA* **99**, 351–358 (2002).
- Kusmartsev, S. & Gabrilovich, D.I. Inhibition of myeloid cell differentiation in cancer: the role of reactive oxygen species. *J. Leukoc. Biol.* **74**, 186–196 (2003).
- Dutz, J.P., Tsomides, T.J., Kageyama, S., Rasmussen, M.H. & Eisen, H.N. A cytotoxic T lymphocyte clone can recognize the same naturally occurring self peptide in association with a self and nonself class I MHC protein. *Mol. Immunol.* **31**, 967–975 (1994).
- Udaka, K., Wiesmuller, K.H., Kienle, S., Jung, G. & Walden, P. Self-MHC-restricted peptides recognized by an alloreactive T lymphocyte clone. *J. Immunol.* **157**, 670–678 (1996).
- Quinn, M.T. The neutrophils respiratory burst oxidase. In *The Neutrophils. New Outlook for Old Cells* (ed. Gabrilovich, D.I.) 35–85 (Imperial College Press, London, 2005).
- Squadrito, G.L. & Pryor, W.A. The formation of peroxynitrite *in vivo* from nitric oxide and superoxide. *Chem. Biol. Interact.* **96**, 203–206 (1995).
- Kusmartsev, S., Nefedova, Y., Yoder, D. & Gabrilovich, D.I. Antigen-specific inhibition of CD8⁺ T cell response by immature myeloid cells in cancer is mediated by reactive oxygen species. *J. Immunol.* **172**, 989–999 (2004).
- Regoli, F. & Winston, G.W. Quantification of total oxidant scavenging capacity of antioxidants for peroxynitrite, peroxy radicals, and hydroxyl radicals. *Toxicol. Appl. Pharmacol.* **156**, 96–105 (1999).
- Balavoine, G.G. & Geletii, Y.V. Peroxynitrite scavenging by different antioxidants. Part I: convenient assay. *Nitric Oxide* **3**, 40–54 (1999).
- Smyth, M. *et al.* Tumor necrosis factor-related apoptosis-inducing ligand (TRAIL) contributes to the interferon- γ -dependent natural killer cell protection from tumor metastasis. *J. Exp. Med.* **193**, 661–670 (2000).
- Kusmartsev, S. & Gabrilovich, D. STAT1 signaling regulates tumor-associated macrophage-mediated T cell deletion. *J. Immunol.* **174**, 4880–4891 (2005).
- Zingarelli, B. *et al.* Oxidation, tyrosine nitration and cytostasis induction in the absence of inducible nitric oxide synthase. *Int. J. Mol. Med.* **1**, 787–795 (1998).
- Haqqani, A.S., Kelly, J.F. & Birnboim, H.C. Selective nitration of histone tyrosine residues *in vivo* in mutant tumors. *J. Biol. Chem.* **277**, 3614–3621 (2002).
- Quint, P., Reutzel, R., Mikulski, R., McKenna, R. & Silverman, D.N. Crystal structure of nitrated human manganese superoxide dismutase: mechanism of inactivation. *Free Radic. Biol. Med.* **40**, 453–458 (2006).
- Wilkinson, I.B., MacCallum, H., Cockcroft, J.R. & Webb, D.J. Inhibition of basal nitric oxide synthesis increases aortic augmentation index and pulse wave velocity *in vivo*. *Br. J. Clin. Pharmacol.* **53**, 189–192 (2002).
- Nikitina, E.Y. *et al.* An effective immunization and cancer treatment with activated dendritic cells transduced with full-length wild-type p53. *Gene Ther.* **9**, 345–352 (2002).
- Pandit, R., Lathers, D., Beal, N., Garrity, T. & Young, M. CD34⁺ immune suppressive cells in the peripheral blood of patients with head and neck cancer. *Ann. Otol. Rhinol. Laryngol.* **109**, 749–754 (2000).
- Bronte, V., Serafini, P., Apolloni, E. & Zanovello, P. Tumor-induced immune dysfunctions caused by myeloid suppressor cells. *J. Immunother.* **24**, 431–446 (2001).
- Melani, C., Chiodoni, C., Forni, G. & Colombo, M.P. Myeloid cell expansion elicited by the progression of spontaneous mammary carcinomas in c-erbB-2 transgenic BALB/c mice suppresses immune reactivity. *Blood* **102**, 2138–2145 (2003).
- Makarenkova, V.P., Bansal, V., Matta, B.M., Perez, L.A. & Ochoa, J.B. CD11b⁺/Gr-1⁺ myeloid suppressor cells cause T cell dysfunction after traumatic stress. *J. Immunol.* **176**, 2085–2094 (2006).
- Mencacci, A. *et al.* CD80⁺Gr-1⁺ myeloid cells inhibit development of antifungal Th1 immunity in mice with candidiasis. *J. Immunol.* **169**, 3180–3190 (2002).
- Atochina, O., Daly-Angel, T., Piskorska, D. & Harn, D. A shistosome expressed immunomodulatory glycoconjugate expand peritoneal Gr1⁺ macrophages that suppress naive CD4⁺ T cell proliferation via an interferon- γ and nitric oxide dependent mechanism. *J. Immunol.* **167**, 4293–4302 (2001).

36. Fahmy, T.M., Bieler, J.G., Edidin, M. & Schneck, J.P. Increased TCR avidity after T cell activation: a mechanism for sensing low-density antigen. *Immunity* **14**, 135–143 (2001).
37. Maile, R. *et al.* Peripheral “CD8 tuning” dynamically modulates the size and responsiveness of an antigen-specific T cell pool in vivo. *J. Immunol.* **174**, 619–627 (2005).
38. Drake, D.R., III, Ream, R.M., Lawrence, C.W. & Braciale, T.J. Transient loss of MHC class I tetramer binding after CD8⁺ T cell activation reflects altered T cell effector function. *J. Immunol.* **175**, 1507–1515 (2005).
39. Alvarez, B. & Radi, R. Peroxynitrite reactivity with amino acids and proteins. *Amino Acids* **25**, 295–311 (2003).
40. De Santo, C. *et al.* Nitroaspirin corrects immune dysfunction in tumor-bearing hosts and promotes tumor eradication by cancer vaccination. *Proc. Natl. Acad. Sci. USA* **102**, 4185–4190 (2005).
41. Sha, W.C. *et al.* Selective expression of an antigen receptor on CD8-bearing T lymphocytes in transgenic mice. *Nature* **335**, 271–274 (1988).
42. Kusmartsev, S. *et al.* All-trans-retinoic acid eliminates immature myeloid cells from tumor-bearing mice and improves the effect of vaccination. *Cancer Res.* **63**, 4441–4449 (2003).
43. Gabrilovich, D.I., Velders, M., Sotomayor, E. & Kast, W.M. Mechanism of immune dysfunction in cancer mediated by immature Gr-1⁺ myeloid cells. *J. Immunol.* **166**, 5398–5406 (2001).